Chloroplast competition is controlled by lipid biosynthesis in evening primroses

Johanna Sobanski[a], Patrick Giavalisco[b], Axel Fischer[c], Julia M. Kreiner[d], Dirk Walther[c], Mark Aurel Schöttler[a], Tommaso Pellizzer[a], Hieronim Golczyk[e], Toshihiro Obata[f], Ralph Bock[a], Barbara B. Sears[g], and Stephan Greiner[a,1]

[a]Department Organelle Biology, Biotechnology and Molecular Ecophysiology, Max Planck Institute of Molecular Plant Physiology, 14476 Potsdam-Golm, Germany; [b]Department Molecular Physiology, Max Planck Institute of Molecular Plant Physiology, 14476 Potsdam-Golm, Germany; [c]Department Metabolic Networks, Max Planck Institute of Molecular Plant Physiology, 14476 Potsdam-Golm, Germany; [d]Department of Ecology & Evolutionary Biology, University of Toronto, ON M5S 3B2, Canada; [e]Department of Molecular Biology, Institute of Biotechnology, John Paul II Catholic University of Lublin, Konstantynów 1I, 20-708, Poland; [f]Center for Plant Science Innovation and Department of Biochemistry, University of Nebraska-Lincoln, Lincoln, NE 68588; and [g]Department of Plant Biology, Michigan State University, East Lansing, MI 48824-1312

In most eukaryotes, organellar genomes are transmitted preferentially by the mother, but molecular mechanisms and evolutionary forces underlying this fundamental biological principle are far from understood. It is believed that biparental inheritance promotes competition between the cytoplasmic organelles and allows the spread of so-called selfish cytoplasmic elements. Those can be, for example, fast-replicating or aggressive chloroplasts (plastids) that are incompatible with the hybrid nuclear genome and therefore maladaptive. Here we show that the ability of plastids to compete against each other is a metabolic phenotype determined by extremely rapidly evolving genes in the plastid genome of the evening primrose *Oenothera*. Repeats in the regulatory region of *accD* (the plastid-encoded subunit of the acetyl-CoA carboxylase, which catalyzes the first and rate-limiting step of lipid biosynthesis), as well as in *ycf2* (a giant reading frame of still unknown function), are responsible for the differences in competitive behavior of plastid genotypes. Polymorphisms in these genes influence lipid synthesis and most likely profiles of the plastid envelope membrane. These in turn determine plastid division and/or turnover rates and hence competitiveness. This work uncovers cytoplasmic drive loci controlling the outcome of biparental chloroplast transmission. Here, they define the mode of chloroplast inheritance, as plastid competitiveness can result in uniparental inheritance (through elimination of the "weak" plastid) or biparental inheritance (when two similarly "strong" plastids are transmitted).

biparental inheritance | selfish cytoplasmic elements | correlation mapping | acetyl-CoA carboxylase | *ycf2*

Most organelle genomes are inherited from the mother (1, 2), but biparental transmission of plastids has evolved independently multiple times. Approximately 20% of all angiosperms contain chloroplasts in the pollen generative cell, indicating at least a potential for biparental transmission (2–4). Although reasons for this are controversial (2, 5–9), a genetic consequence of the biparental inheritance patterns is a genomic conflict between the two organelles. When organelles are transmitted to the progeny by both parents, they compete for cellular resources. As the plastids do not fuse and hence their genomes do not undergo sexual recombination, selection will favor the organelle genome of the competitively superior plastid (2, 10–13). In a population, the ensuing "arms race" can lead to evolution and spread of selfish or aggressive cytoplasmic elements that potentially could harm the host cell. The mechanisms and molecular factors underlying this phenomenon are elusive, yet there is solid evidence for a widespread presence of competing organelles (2). Heteroplasmic cells can be created from cell fusion events, mutation of organelle DNA, or sexual crosses (14–17), but only very few cases have been studied in some detail in model organisms. One them is *Drosophila*, in which mitochondrial competition experiments can be set up via cytoplasmic microinjections (18, 19). Another is the evening prim-

rose (genus *Oenothera*) (20, 21). This plant genus is certainly the model organism of choice to study chloroplast competition; the original theory of "selfish" cytoplasmic elements is based on evening primrose genetics (10): in the *Oenothera*, biparental plastid inheritance is the rule (22), and the system is a prime example of naturally occurring aggressive chloroplasts (2, 10). Based on extensive crossing studies, five genetically distinguishable chloroplast genome (plastome) types were shown to exist. Those were designated by Roman numerals (I–V) and grouped into three classes according to their inheritance strength or assertiveness rates in crosses (strong, plastomes I and III; intermediate, plastome II; and weak, plastomes IV and V), reflecting their ability to outcompete a second chloroplast genome in the F1 generation upon biparental transmission (20, 22, 23). The plastome types were initially identified based on their (in)compatibility with certain nuclear genomes (24, 25). Strong plastomes provide "hitchhiking" opportunities for

Significance

Plastids and mitochondria are usually uniparentally inherited, typically maternally. When the DNA-containing organelles are transmitted to the progeny by both parents, evolutionary theory predicts that the maternal and paternal organelles will compete in the hybrid. As their genomes do not undergo sexual recombination, one organelle will "try" to outcompete the other, thus favoring the evolution and spread of aggressive cytoplasms. The investigations described here in the evening primrose, a model species for biparental plastid transmission, have discovered that chloroplast competition is a metabolic phenotype. It is conferred by rapidly evolving genes that are encoded on the chloroplast genome and control lipid biosynthesis. Because of their high mutation rate, these loci can evolve and become fixed in a population very quickly.

loci that result in incompatible or maladaptive chloroplasts, and these would be viewed as selfish cytoplasmic elements (2, 10). It was further shown that the loci, which determine the differences in competitive ability of the chloroplast, are encoded by the chloroplast genome itself (20, 22, 23).

Results

To pinpoint the underlying genetic determinants, we developed an association mapping approach that correlates local sequence divergence to a phenotype. We analyzed 14 complete chloroplast genomes from *Oenothera* WT lines, whose inheritance strength had been previously classified in exhaustive crossing analyses (20, 22, 26). This enabled us to correlate the experimentally determined inheritance strengths to sequence divergence in a given alignment window (*Materials and Methods* and *SI Appendix, SI Text*). The Pearson's and Spearman's applied correlation metrics associated the genetic determinants of inheritance strength with four major sites: the regulatory region of the fatty acid biosynthesis gene *accD* (promoter, 5′-UTR, and protein N terminus), the *origin of replication B* (*oriB*), *ycf1*, and *ycf2* (including its
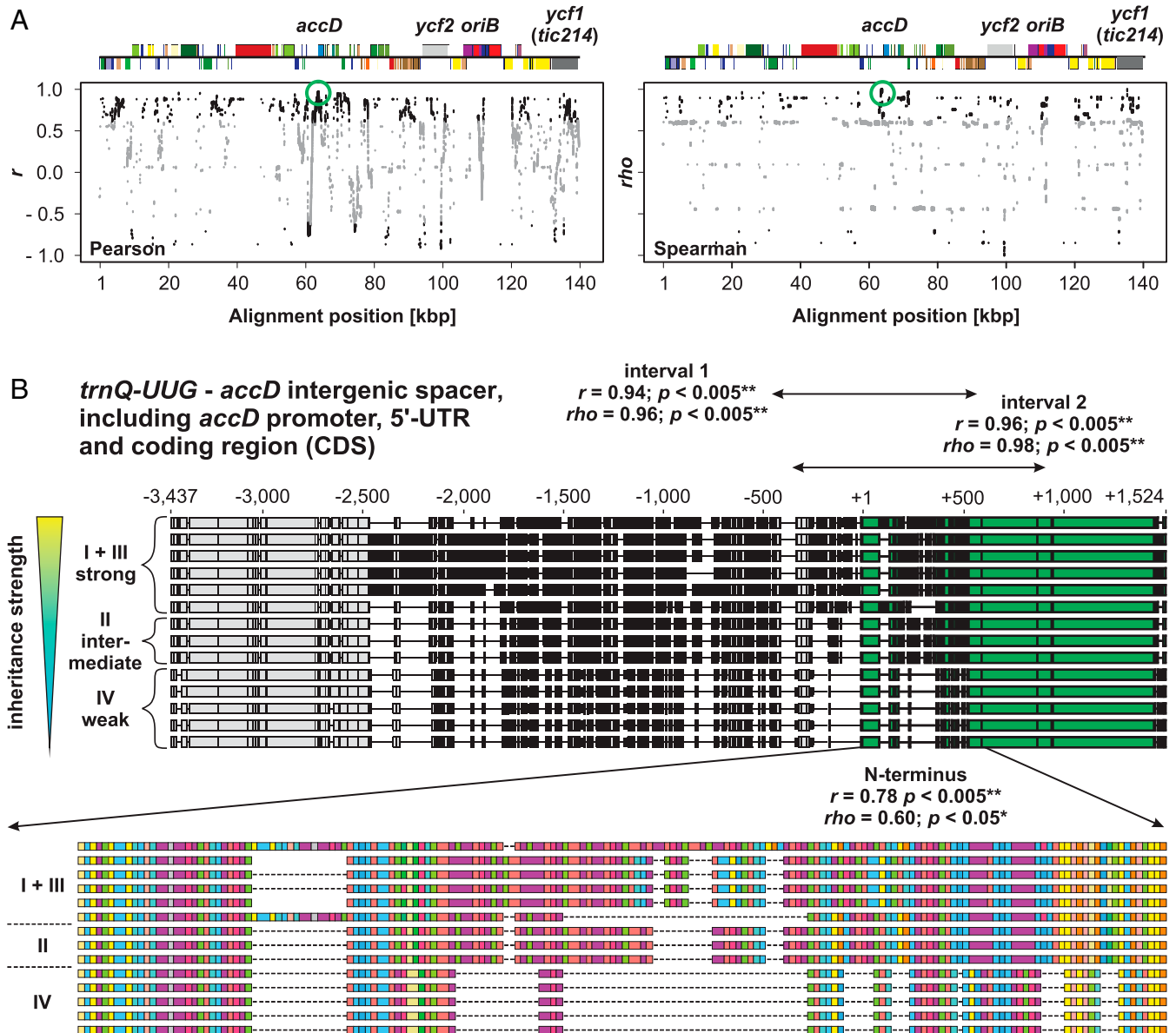

Fig. 1. Correlation mapping to identify chloroplast loci for inheritance strength in the WT chloroplast genomes. (*A*) Spearman and Pearson correlation to inheritance strength plotted against alignment windows of the WT plastomes. Relevant genes or loci with significant correlation are indicated in the linear plastome maps above. The region displayed in *B* is highlighted by green circles. Significant correlations (*P* < 0.05) are shown in black. Correlations to *k*-means classes are shown. Further details are provided in *Materials and Methods*, *SI Appendix, SI Text*, and main text. (*B*) Correlation to inheritance strength at the *accD* region in the WT plastomes. Individual sequences are sorted according to their competitive ability. Polymorphic regions are indicated in black, and thin lines represent gaps mostly resulting from deletions. (*Upper*) Alignment of the *trnQ–UUG–accD* intergenic spacer (−3,437 to −1) and the *accD* gene, including promoter, 5′-UTR, and CDS. The *accD* CDS, starting from +1, is highlighted in green. Regions marked by "interval 1" and "interval 2" display nearly absolute correlation to inheritance strength (*SI Appendix, SI Text* and Dataset S1). Note that these sequence intervals span the promotor region, the 5′-UTR, and the 5′-end of *accD*. All three are considered to play a regulatory role (29, 75–78). (*Lower*) Amino acid sequence of the AccD N terminus and correlation to inheritance strength. Colors indicated different amino acids. Most variation in the sequence is conferred by repeats encoding glutamic acid-rich domains marked in purple (*SI Appendix, SI Text*).

promoter/5′-UTR; Fig. 1 and *SI Appendix, SI Text, Fig. S1, and Dataset S1*). The *ycf1* and *ycf2* genes are two ORFs of unknown function; *ycf1* (or *tic214*) has tentatively been identified as an essential part of the chloroplast protein import machinery (27), but this function has been questioned (28). The *accD* gene encodes the β-carboxyltransferase subunit of the plastid-localized plant heteromeric acetyl-CoA carboxylase (ACCase). The enzyme is responsible for catalyzing the initial tightly regulated and rate-limiting step in fatty acid biosynthesis. The other three required ACCase subunits, α-carboxyltransferase, biotin-carboxyl carrier protein, and biotin carboxylase, are encoded by nuclear genes (29). The polymorphisms detected through our correlation mapping represent large insertions/deletions (indels), which are in frame in all coding sequences (CDSs; Fig. 1*B* and *SI Appendix, SI Text, Figs. S2–S6, and Dataset S2*). Several other polymorphisms in intergenic spacers of photosynthesis and/or chloroplast translation genes were correlated with plastome assertiveness rates (Fig. 1*A* and *SI Appendix, SI Text and Dataset S1*). However, both of those gene classes are unlikely to affect chloroplast inheritance, as other studies have shown that mutations in genes that result in chlorophyll-deficient chloroplasts do not alter their inheritance strengths in the evening primrose (20, 30, 31) (*SI Appendix, SI Text*). By contrast, the large

ORFs of unknown function, the origins of replication, and a central gene in lipid metabolism such as *accD* (29) are serious candidates to encode factors involved in chloroplast competition.

Because of the lack of measurable sexual recombination in seed plant chloroplast genomes (2), our correlation mapping method first established associations of polymorphic loci that are fixed in the slow plastome type IV with weak inheritance strength, regardless of their functional relevance (*SI Appendix, SI Text*). Ideally, this problem can be partially circumvented if phylogenetic independence of the correlation between inheritance strength and a sequence's window comprising a candidate locus can be shown. Therefore, to correct for phylogeny in our correlation mapping analysis, we implemented phylogenetic generalized least squares (PGLS). This, however, yielded insignificant results after *P* value adjustment when applied to all sequence windows of the WT plastomes (*SI Appendix, SI Text, Fig. S1, and Dataset S1*). Because the correlation mapping results did not withstand controlling for phylogeny and multiple testing, we aimed to generated mutants from the candidate loci to test whether those loci affect inheritance strength. For this, we conducted a genetic screen for weak chloroplast mutants derived from the strong chloroplast genome I by employing a *plastome*
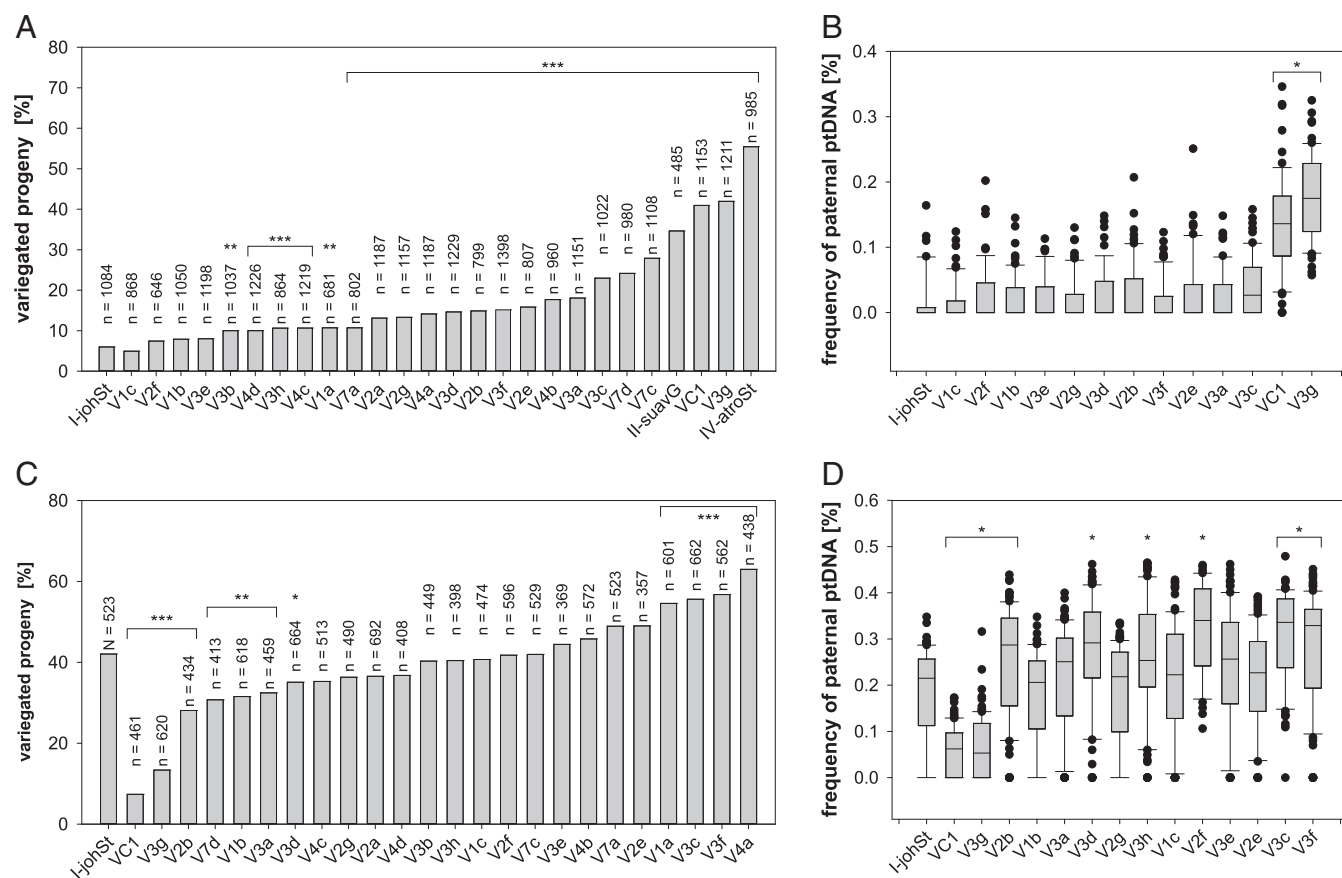
Fig. 2. Transmission efficiencies of plastome I variants and the WT plastomes I-johSt (strong), II-suavG (intermediate), and IV-atroSt (weak) as determined by crosses with I-chi/I-hookDV (strong) and IV-delta/IV-atroSt (weak). (*A* and *C*) Classical approach based on counting of variegated seedlings. (*B* and *D*) MassARRAY assay quantifying maternal and paternal ptDNA. WTs and green variants were crossed as the seed parent to I-chi as male parent (*A*) and as the pollen parent to IV-delta as female parent (*C*). The *X*-axis depicts the average percentage of variegated progeny (percentage biparental inheritance) obtained from three seasons (2013, 2014, and 2015). Fisher's exact test determined significance of differences between variants and their progenitor I-johSt (***$P < 0.0001$, **$P < 0.001$, *$P < 0.01$). Crosses of I-johSt and variants with I-hookDV as male (*B*) and with IV-atroSt as female parent (*D*). Box plots represent the transmission frequencies of the paternal plastomes measured by MassARRAY. To account for significant differences vs. I-johSt, Kruskal–Wallis one-way ANOVA on ranks was performed (*$P < 0.05$). Because of the detection threshold of the MassARRAY (5–10%), most variants show the same or slightly decreased transmission efficiency as their WT I-johSt (*B* and *D*). Only for the weak variants VC1 and V3g is the difference of the ratio of paternal and maternal ptDNA in the pool large enough to result in the detection of a significantly lower assertiveness rate in both crossing directions. Altogether, the classical approach using bleached chloroplast mutants gives more reliable results and allows a much finer discrimination of transmission efficiencies (cf. *A* vs. *B* and *C* vs. *D*). Further details are provided in *SI Appendix, SI Text*.

mutator (*pm*) allele (*Materials and Methods*). The *pm*-based mutagenesis approach yields indels in repetitive regions (32), similar to those identified by our association mapping (*SI Appendix, SI Text*). This led to the isolation of 24 plastome I variants with altered inheritance strength (Fig. 2 and *SI Appendix, SI Text*). As we selected for green and photosynthetically competent chloroplasts in the mutagenesis (*Materials and Methods*), none of those variants differed from the WT in their photosynthetic parameters, chloroplast size, or chloroplast volume per cell. The plants with the variant plastomes did not display any growth phenotype (*SI Appendix, SI Text* and Figs. S7–S9). Sequence analysis of 18 variants, spanning the range of observed variation in inheritance strength, revealed an average of seven mutation events per variant. The analysis included one additional variant (VC1) with more background mutations, which resulted from its isolation after being under the mutagenic action of the *pm* for several generations (*Materials and Methods* and *SI Appendix, SI Text*). Most of the *pm*-induced mutations are composed of single base pair indels at oligo(N) stretches in intergenic regions, i.e., not of functional relevance, or larger in-frame indels at the highly repetitive sites of *accD*, *ycf1*, *ycf2*, or *oriB* (*SI Appendix, Figs. S2–S6, Table S1, and Dataset S2*). Correlation analysis to inheritance strengths at these sites confirmed the relevance of *accD* and *ycf2* in chloroplast inheritance ($r = 0.72$, $P = 0.05$ for the 5′ end of AccD; $r = 0.91$, $P < 0.0005$ for the promotor/5′-UTR of *ycf2*; and $r = 0.70$, $P < 0.005$ for a mutated site in Ycf2; Fig. 3 and *SI Appendix, SI Text* and Figs. S2–S6 and S10). These findings were confirmed by two additional very weak mutants derived from the strong plastome III (*Materials and Methods* and *SI Appendix, SI Text*). Based on the full chloroplast genome sequences of these lines (*SI Appendix, Dataset S2*), it appeared that the promotor/5′-UTR of *accD* is affected in one of the lines. In addition, in both lines, the *ycf2* gene is most heavily mutated compared with all other (weak) materials sequenced so far. This strongly advocates for *ycf2* being involved in chloroplast competition (*SI Appendix, Table S2*). The very weak variants of plastome III, as well as correlation analysis of *oriB* and *ycf1* in the plastome I variants, did not support an involvement of these regions in the inheritance phenotype (Fig. 3 and *SI Appendix, SI Text*, Figs. S6 and S10, and Tables S1 and S2). Furthermore, the second replication origin (*oriA*) was found to be nearly identical within all sequenced WT or mutant plastomes.

These data argue against plastid DNA (ptDNA) replication, per se, being responsible for differences in chloroplast competitiveness. This conclusion is in line with previous analyses of the *Oenothera* replication origins, which had suggested that their variability does not correlate with the competitive strength of the plastids (33, 34) (*SI Appendix, SI Text*). We further confirmed this by determining the relative ptDNA amounts of chloroplasts with different inheritance strengths in a constant nuclear background. No significant variation of ptDNA amounts was observed over a developmental time course in these lines, thus excluding ptDNA stability and/or turnover as a potential mechanism (*SI Appendix, SI Text* and Fig. S11). Moreover, no significant differences in nucleoid numbers per chloroplast or nucleoid morphology was observed, as judged by DAPI staining (*SI Appendix, SI Text* and Figs. S12 and S13).

Next, we conducted a more detailed analysis of *accD* and *ycf2*. In a constant nuclear background, the weak WT plastome IV appeared to be an *accD* overexpressor compared with the strong WT plastome I, as judged from Northern blot analyses. However, this overexpression could not be detected in the plastome I variants that have a weakened competitive ability. Similar results were obtained for *ycf2*, which has an RNA of approximately 7 kb, reflecting the predicted size of the full-length transcript (*SI Appendix, SI Text* and Fig. S14). Interestingly, lower bands, probably reflecting transcript processing and/or degradation intermediates, differ between the strong WT plastome I and the weak WT plastome IV, with the latter being similar to the weak plastome I variants.

As these analyses did not allow conclusions about the functionality of AccD or Ycf2 in our lines, we decided to determine the ACCase activity in chloroplasts isolated from a constant nuclear background. As shown in Fig. 4*A*, the presence of large mutations/polymorphisms in the N terminus of the *accD* reading frame co-occurs with higher levels of ACCase enzymatic activity. Surprisingly, mutations/polymorphisms in *ycf2* also have an influence on ACCase activity, as revealed by lines that are not affected by mutations in *accD*. The molecular nature of this functional connection between Ycf2 and ACCase activity is currently unclear, although Ycf2 shares weak homologies to the FtsH protease (35, 36), which has a regulatory role in lipopolysaccharide synthesis in *Escherichia coli* (37). In any case, a simple relationship of ACCase activity and competitive ability of plastids is not present, but alterations in the earliest step of fatty acid biosynthesis can conceivably result in various changes in lipid metabolism (*SI Appendix, SI Text*).

To examine the alterations in lipid biosynthesis, we determined the lipid composition of seedlings harboring strong and weak WT chloroplasts as well as the variants that differ in chloroplast inheritance strength (*SI Appendix, SI Text* and Table S3). Then, we employed a least absolute shrinkage and selection operator (LASSO) regression model to predict competitive ability of a given chloroplast (Fig. 4*B*). As chloroplast inheritance strength is independent of photosynthetic competence (*SI Appendix, SI Text*), we included pale lines. The aim was to enrich the lipid signal responsible for inheritance strength, i.e., to deplete for structural lipids of the photosynthetic thylakoid membrane, which is a major source of chloroplast lipids (38). Indeed, of 102 lipids analyzed, 20 predictive ones for inheritance strengths were identified (Fig. 4*C* and *SI Appendix, SI Text* and Table S4). Strikingly, the signal is independent of greening (i.e., an intact thylakoid membrane system and the photosynthetic capacity), which is in line with the genetic data (*SI Appendix, SI Text*). This result hints at the chloroplast envelope determining assertiveness rates, a view that is supported by the fact that half of the predictive lipids come from lipid classes present in plastidial membranes and abundant in the chloroplast envelope, such as MGDG, DGDG, PG, and PC (39). The remaining predictive lipids mostly represent storage lipids (TAG). This might be a result of an altered fatty acid pool (*SI Appendix, SI Text*). Statistical significance of enrichment of a given class could not be established as a result of low numbers (*SI Appendix, SI Text* and Tables S4 and S5), although, especially in the lipid class PC, which is the dominant phospholipid class in the chloroplast outer envelope (40), 4 of 13 detected lipids were found to be predictive. In the chloroplast, PCs are specific to the envelope membrane and essentially absent from thylakoids. This makes it very likely that the lipid composition of the envelope membrane affects chloroplast competition. A possible explanation could be that strong and weak chloroplasts differ in division rates, for example, as a result of differential effectiveness in recruiting chloroplast division rings, which are anchored by membrane proteins (41). Alternatively, chloroplast stability might depend on envelope membrane composition. Strictly speaking, we cannot exclude a (further) involvement of extraplastidial membranes to the inheritance phenotype (most of the total cellular PCs are found in the ER and the plasma membrane) (38), but this would require a much more complicated mechanistic model.

Discussion

The present work explains plastid competition following biparental inheritance from a mechanistic perspective and points to genetic loci that appear to be responsible for these differences. Moreover, as chloroplast competition can result in uniparental inheritance through the elimination of weak
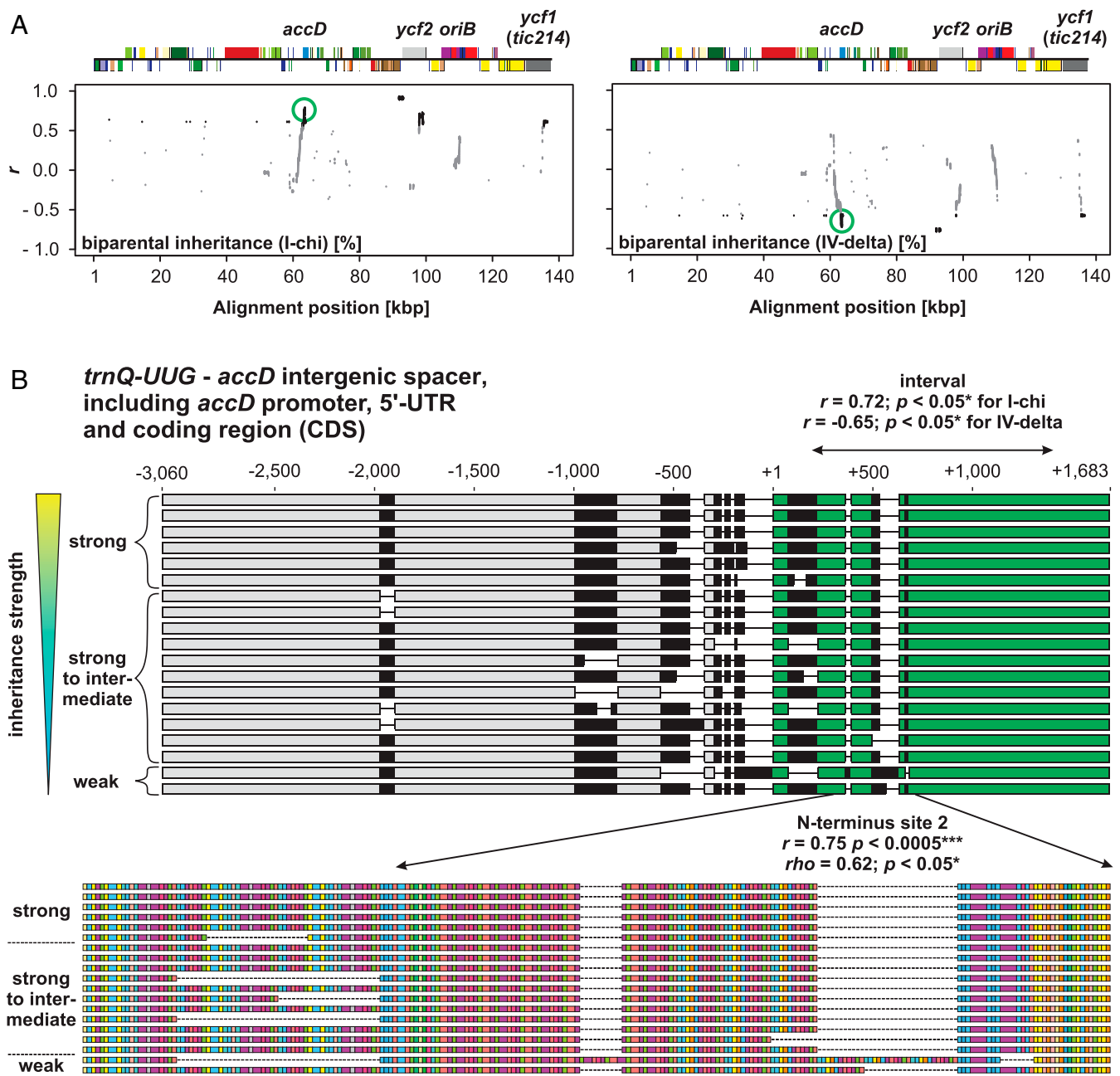
Fig. 3. Correlation mapping to identify chloroplast loci for inheritance strength in the plastome I variants. (*A*) Pearson correlation to inheritance strength plotted against alignment windows of the variants' plastomes. Relevant genes or loci with significant correlation are indicated in the linear plastome maps above. The region displayed in *B* is highlighted by green circles. Significant correlations ($P < 0.05$) are shown in black. Correlations to I-chi and IV-delta crosses (Fig. 2 *A* and *C*) are shown. Further details are provided in *Materials and Methods*, *SI Appendix, SI Text*, and main text. (*B*) Correlation to inheritance strength at the *accD* region in the variants' plastomes. Individual sequences are sorted according to their competitive ability. Polymorphic regions are indicated in black, and thin lines represent gaps mostly resulting from deletions. (*Upper*) Alignment of the *trnQ–UUG–accD* intergenic spacer (−3,060 to −1) and the *accD* gene, including promoter, 5′-UTR, and CDS. The *accD* CDS, starting from +1, is highlighted in green. The region marked by "interval" within the *accD* CDS displays high correlation to inheritance strength (*SI Appendix, SI Text* and Dataset S1). (*Lower*) Amino acid sequence of the AccD N terminus and correlation to inheritance strength. Colors indicate different amino acids. Most variation in the sequence is conferred by repeats encoding glutamic acid-rich domains marked in purple (*SI Appendix, SI Text*).

chloroplasts (9, 20, 30), at least for the evening primrose, the mechanistic explanation can be extended to uniparental transmission. Because approximately 20% of all angiosperms contain ptDNA in the sperm cell, it is likely that this mechanism is present in other systems (3, 5, 42). However, it should be emphasized that uniparental inheritance can be achieved by multiple mechanisms (2), and nuclear loci controlling the mode of organelle inheritance still need to be identified.

Arguably, the most surprising finding from our work is the discovery that chloroplast competition in evening primroses is essentially a metabolic phenotype and not directly connected to ptDNA replication or copy number (43). The underlying molecular loci are rapidly evolving genes throughout the plant kingdom. In general, the Ycf1 and Ycf2 proteins as well as the N terminus of AccD are highly variable in angiosperms (44–46). Interactions between them were repeatedly suggested (46, 47);
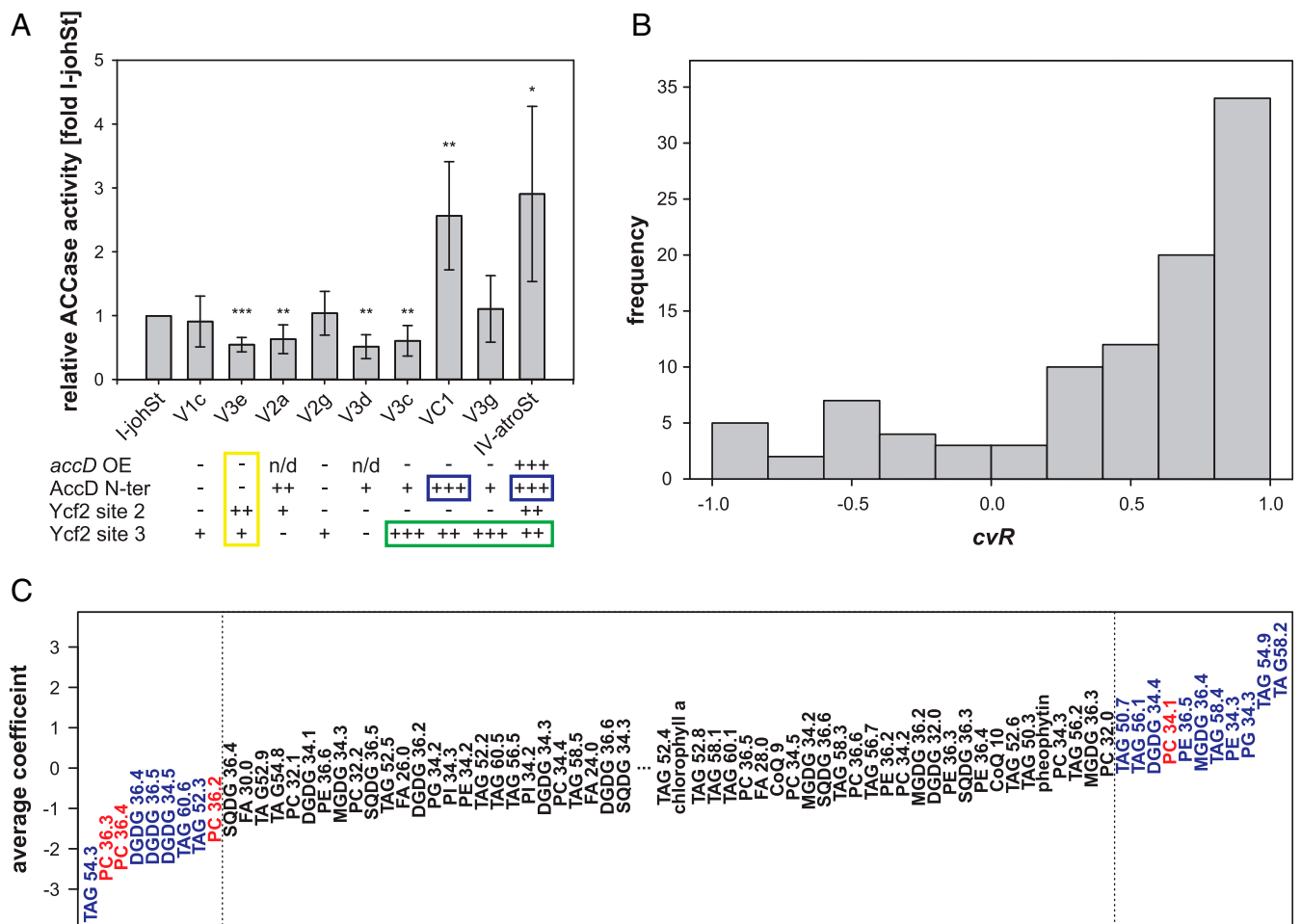
Fig. 4. ACCase activity and prediction of inheritance strengths based on lipid level. (*A*) ACCase activity of chloroplasts with difference inheritance strengths sorted according to competitive abilities (percentage biparental inheritance I-chi; cf. Fig. 2); *accD* OE, *accD* overexpressor; AccD N-ter, AccD N terminus (*SI Appendix, SI Text*). Compared with I-johSt, −, not affected; +, mildly affected; ++, intermediately affected; +++, strongly affected; n/d, not determined (cf. *SI Appendix*, Figs. S1–S5 and S14). Note the influence of mutations in *ycf2* on AccD activity in a nonmutated *accD* background (yellow box), the striking co-occurrence of mutations in the AccD N terminus with ACCase activity (blue boxes), and co-occurrence of large mutations/polymorphisms in site 3 of Ycf2 with inheritance strengths (green box). Significance of difference compared with I-johSt was calculated by using a paired two-tailed *t* test (***P < 0.0005, **P < 0.005, and *P < 0.05). (*B*) Histogram of Pearson correlation coefficient *cvR* between actual and predicted inheritance strengths obtained from 100 cross-validation runs. Note the shift toward 1.0, pointing to the predictive power of lipid data in the LASSO regression model. (*C*) Average linear LASSO model coefficients of the 102 lipids/molecules available for analysis (cf. *SI Appendix*, Table S4). The 20 identified predictive lipids are marked in color. PCs, the dominant phospholipids of the chloroplast outer envelope, are indicated in red. In general, large absolute values show predictive power negatively or positively correlating with inheritance strength. Predictive lipids were designated when their absolute average weight was greater than 1 SD of all weight values obtained for the 102 lipids. For better presentability, lipids/molecules with an absolute average weight ~0.00 were removed from the figure.

e.g., the loss of *ycf1*, *ycf2*, and *accD* genes from the plastome of grasses (48), as well as their common retention in many plastomes of nonphotosynthetic parasites (49), provides room for speculation about functional interaction (46). In addition, *Silene*, a genus in which biparental chloroplast transmission is described (50), exhibits accelerated evolution of *accD* (51). In contrast, *Campanulastrum*, again displaying biparental chloroplast inheritance (9), has lost *accD* from the chloroplast genome, and its *ycf2* is under accelerated evolution (52). In pea, which usually shows uniparental chloroplast inheritance, one strain with biparental chloroplast inheritance exists, and biparental transmission is accompanied by chloroplast/nuclear genome incompatibility in the resulting hybrid (53), with repeats in *accD* implicated as being responsible (54). Analysis of a very similar chloroplast/nuclear genome incompatibility in *Oenothera* also identifies repeats in *accD* as causative (55). Hence, correlation of the highly divergent *accD* gene (and/or *ycf2*) with the presence or absence of biparental inheritance and/or chloroplast incompatibility is certainly worth investigating on a broader phylogenetic scale. Connected with that, the *accD* plastome variants represent a superb material to study ACCase regulation and those of its nuclear counterparts. Interaction effects in different nuclear genomic background should be observable.

In the plastome of the evening primrose, the loci involved in chloroplast competition are very sensitive to replication slippage as a result of the presence of highly repetitive sequences, and that process appears to be the major mechanism of spontaneous chloroplast mutation (31, 44) (*SI Appendix, SI Text*). This result is somewhat reminiscent of recent findings in *Drosophila* in which sequence variation in the noncoding regulatory region of the mitochondrial genome, containing the origins of replication, was associated with different competitive abilities. Similar to *Oenothera*, these sequences are highly repetitive and hypervariable and contribute to cytoplasmic drive. In *Drosophila*, they are among the most divergent ones in Metazoa, pointing to their positive selection (19) (*SI Appendix, SI Text*).

Our analyses show that, as a result of their high mutation rates, cytoplasmic drive loci can evolve and become fixed in a population very quickly: in *Oenothera*, the current view on the evolutionary history of the plastome is IV → II → I/III (56), with an estimated divergence time of ∼830,000 y (44). This is largely based on chloroplast/nuclear incompatibility and can explain why plastomes IV and II (although compatible with the nuclear genomes of many *Oenothera* species) were outcompeted by the newly evolved aggressive plastomes I and III in many species. Interestingly, the extant plastomes I and III do not form a phylogenetic clade. The recently evolved strong plastome I clusters with the intermediately strong plastome II, with recently evolved plastome III as outgroup (*SI Appendix*, Fig. S1*B*). The divergence time of II and III, however, is only approximately 420,000 y (44). Hence, evolution and fixation of an aggressive cytoplasm happened twice independently within a very short time frame.

Materials and Methods

Plant Material. Throughout this work, the terms "*Oenothera*" or "evening primrose" refer to subsection *Oenothera* (genus *Oenothera* section *Oenothera*) (56). Plant material used here is derived from the *Oenothera* germplasm collection harbored at the Max Planck Institute of Molecular Plant Physiology (Potsdam-Golm, Germany) (57). Part of this collection is the so-called Renner Assortment, a collection of lines thoroughly characterized by the genetic school of Otto Renner (22, 58). Therefore, the original material of Schötz (21, 26), which determined the classes of chloroplast replication speeds, was available for correlation mapping (as detailed later). For all other genetic or physiological work presented here, the nuclear genetic background of *Oenothera elata* subsp. *hookeri* strain johansen Standard (59) was used. The employed chloroplast (genomes) are native or were introgressed into that race by author S.G. or Wilfried Stubbe. The WT chloroplast genomes (I-johSt, I-hookdV, II-suavG, and IV-atroSt) are compatible with, and hence green when combined with, the johansen Standard nucleus. The chloroplast genome III-lamS confers a reversible bleaching, so-called virescent, phenotype in this genetic background (56, 60) (*SI Appendix*, Fig. S15). The white chloroplast mutants I-chi and IV-delta (*SI Appendix*, Fig. S15) are part of the huge collection of spontaneous plastome mutants compiled by Stubbe and coworkers (31, 61, 62). Both mutants harbor a similar single locus mutation in the *psaA* gene (encoding a core subunit of photosystem I) and derive from the strong and weak WT plastomes I-hookdV and IV-atroSt, respectively (31). *SI Appendix*, Tables S6–S11 provide a summary of all strains and origins of the chloroplast genomes, including the *pm*-induced variants that are subsequently described.

Plastome Mutator Mutagenesis. The *pm* line is a descendant of the original isolate E-15–7 of Melvin D. Epp. The nuclear *pm* allele was identified after an ethyl methanesulfonate mutagenesis (63) in johansen Standard. When homozygous, the *pm* causes a 200–1,000× higher rate of chloroplast mutants compared with the spontaneous frequency. The underlying mutations mostly represent indels resulting from replication slippage events (32, 63–66).

Johansen Standard plants newly restored to homozygosity for the nuclear *pm* allele (*pm/pm*) were employed to mutagenize the chloroplast genome (I-johSt) as described previously (35). Homozygous *pm* plants were identified when new mutant chlorotic sectors were observed on them. On those plants, flowers on green shoots were backcrossed to the WT *PM* allele as pollen donor. In the resulting *pm/PM* populations, the chloroplast mutations were stabilized. This led (after repeated backcrosses with the *PM* allele and selection with appropriate markers against the paternal chloroplast) to homoplasmic green variants derived from the strong plastome I-johSt. The variants differ by certain indels or combination of indels, and the material was designated V1a, V1b, V2a, etc., where "V" stands for variant, the Arabic number for the number of the backcrossed plant in the experiment, and the small Latin letter for the shoot of a given plant. An additional line, named VC1, was derived from a similar *pm* mutagenesis of I-johSt, but the mutagenesis was conducted over several generations. Therefore, VC1, which is also a green variant, carries a much larger number of background mutations than do variants V1a, V1b, V2a, etc. (*SI Appendix*, Table S10). The two variant chloroplast genomes III-V1 and III-V2 (*SI Appendix*, Table S11) have a derivation similar to VC1. They are derived from the strong WT chloroplast genome III-lamS, which displays a reversible bleaching (virescent phenotype) in the johansen Standard nuclear genetic background. To mutagenize this

chloroplast genome, it was introgressed into the *pm/pm* background of johansen Standard by Wilfried Stubbe and self-pollinated for a number of generations. When stabilized with the *PM* allele, it still displayed a virescent phenotype that is comparable to the original WT plastome III-lamS (*SI Appendix*, Fig. S15). Both lines quite likely go back to the same ancestral *pm/pm*-johansen Standard III-lamS plant, i.e., experienced a common mutagenesis before separating, although the number of (independent) mutagenizing generations is unclear.

Determination of Plastid Inheritance Strength. In the evening primroses, biparental transmission of plastids shows maternal dominance, i.e., F1 plants are homoplasmic for the maternal chloroplast or heteroplasmic for the paternal and maternal chloroplasts. If, in such crosses, one of the chloroplasts is marked by a mutation, resulting in a white phenotype, the proportion of variegated (green/white; i.e., heteroplasmic) seedlings can be used to determine chloroplast inheritance strength (as percentage of biparental inheritance). Moreover, if, in such crosses, one of the crossing partners is kept constant, the inheritance strength of all tested chloroplasts with respect to the constant one can be determined (20, 21, 26, 30). For example, in the I-chi crosses (in which the strong white plastid is donated by the father, as detailed later), more variegated seedlings are found in the F1, indicating that more paternal (white) chloroplasts were able to outcompete the dominating maternal green chloroplasts. Hence, in this crossing direction, small biparental percentage values indicate strong (i.e., assertive) plastomes from the maternal parent and high biparental values indicate weak variants contributed by the maternal parent. The situation is reversed in the reciprocal cross in which the white chloroplast is donated by the mother, as is the case in the IV-delta crosses. Here, the weak white chloroplast is maternal, and strong green variants contributed by the pollen give high fractions of variegated plants in the F1, whereas low percentages of biparental progeny result when weak green variants are carried by the pollen donor.

Crossing Studies. All crossing studies between chloroplast genomes were performed in the constant nuclear background of the highly homozygous johansen Standard strain (as described earlier). Germination efficiency in all populations was 100% (*SI Appendix, Supplementary Materials and Methods*). Transmission efficiencies of the green plastome I variants (V1a, V1b, V2a, etc.) were determined by using the white chloroplast I-chi (strong inheritance strength) and IV-delta (weak inheritance strength) as crossing partners, respectively. This allows the determination of the inheritance strength of a given green chloroplast relative to a white one based on quantification of the biparental (variegated) progeny among the F1, as progeny that inherit chloroplasts from only the paternal parent are virtually nonexistent (*SI Appendix, SI Text*). The fraction of variegated (green/white) seedlings was assessed in the I-chi crosses in which the white mutant was contributed by the paternal parent. Similarly, variegated (white/green) seedlings were quantified in the IV-delta crosses in which the white mutant was donated by the maternal parent (21, 26, 30) (as described earlier). In the I-chi crosses, the green plastome I variants, as well as the WT chloroplast genomes I-johSt (strong inheritance strength; native in the genetic background of johansen Standard and the original WT chloroplast genome used for mutagenesis), II-suavG (intermediate inheritance strength), and IV-atroSt (weak inheritance strength) were crossed as female parent to I-chi in three following seasons (2013, 2014, and 2015). In the IV-delta crosses, green variants and I-johSt were crossed as male parent to IV-delta, again in three independent seasons, 2013, 2014, and 2015. From each cross of each season, randomized populations of 100–300 plants were grown twice independently, followed by visual assessment of the number of variegated seedlings/plantlets 14–21 d after sowing (DAS; I-chi crosses) or 7–14 DAS (IV-delta crosses). Based on these counts, the percentage of variegated progeny was calculated for each individual cross. To determine statistically significant differences between the transmission efficiencies of the plastome I variants and I-johSt, the numbers from all three seasons were summed for a particular cross and a Fisher's exact test was employed.

A very similar experiment was performed to determine the inheritance strength of the two variants III-V1 and III-V2 (*SI Appendix, SI Text*), which derive from the strong chloroplast genomes III-lamS. Here, in two independent seasons (2015 and 2016), the WT I-johSt was used as pollen donor to induce variegation between the maternal plastome III (giving rise to a virescent phenotype) and the green plastome I (native in the background of johansen Standard as described earlier).

To determine transmission efficiencies independent of white chloroplast mutants or other bleached material, the plastome I variants (including their WT I-johSt) were crossed to the green WT plastomes IV-atroSt (weak inheritance strength) as female parent and to I-hookdV (strong inheritance

strength) as male parent in two independent seasons (2013 and 2014). F1 progeny was harvested at 6 DAS by pooling 60–80 randomized seedlings, and the ratios of the plastome types in the pool were analyzed via MassARRAY (Agena Bioscience) as described in the following section.

MassARRAY: Multiplexed Genotyping Analysis Using iPlex Gold. SNP genotyping to distinguish plastome I-johSt and I-hookdV/I-chi or I-johSt and IV-atroSt/IV-delta and subsequent quantification of their plastome ratios in appropriate F1s was carried out with the MassARRAY system (Agena Bioscience). The system was used to analyze chloroplast transmission efficiencies in different crosses. For this, total DNA was prepared from 60–80 randomized pooled plantlets at 6 DAS. Then, 10 SNPs distinguishing the plastomes I-johSt and I-hookdV/I-chi (I/I assay) and 15 SNPs between I-johSt and IV-atroSt/IV-delta (I/IV assay) were selected. Two appropriate primers flanking the SNP and one unextended primer (binding an adjacent sequence to the SNP) were designed by using MassARRAY Assay Design v4.0 (Agena Bioscience). Primer sequences and SNPs and their positions in I-johSt are listed in *SI Appendix*, Table S12. Plastome regions were amplified in a 5-μL PCR containing PCR buffer (2 mM MgCl$_2$, 500 μM dNTP mix, 1 U HotStartTaq; Agena Bioscience), 10 ng DNA, and 10 (I/I assay) or 15 (I/IV assay) PCR primer pairs, respectively, at concentrations ranging from 0.5 to 2.0 μM. The reaction mix was incubated for 2 min at 95 °C in 96-well plates, followed by 45 cycles of 30 s at 95 °C, 30 s at 56 °C, and 60 s at 72 °C, and a final elongation for 5 min at 72 °C. Excess nucleotides were removed by adding 0.5 U shrimp alkaline phosphatase (SAP) enzyme and SAP buffer (Agena Bioscience), followed by an incubation for 40 min at 37 °C and 5 min at 85 °C. For the primer extension reaction, the iPLEX reaction mixture (containing Buffer Plus, Thermo Sequenase, and termination mix 96; Agena Bioscience) and, depending on the primer, the extension primers at a concentration of 7–28 μM were added. Sequence-specific hybridization and sequence-dependent termination were carried out for 30 s at 94 °C, followed by 40 cycles of 5 s at 94 °C plus five internal cycles of 5 s at 52 °C and 5 s at 80 °C, and finally 3 min at 72 °C. After desalting with CLEAN resin (Agena Bioscience), the samples were spotted on 96-pad silicon chips preloaded with proprietary matrix (SpectroCHIP; Agena Bioscience) by using the Nanodispenser RS1000 (Agena Bioscience). Subsequently, data were acquired with a MALDI-TOF mass spectrometer MassARRAY Analyzer 4 (Agena Bioscience) and analyzed with the supplied software. To identify significant differences in the frequencies of paternal ptDNA, Kruskal–Wallis one-way ANOVA on ranks was performed.

k-Means Clustering to Classify Inheritance Strength. For the WT chloroplasts, inheritance strength was classified by using the biparental transmission frequencies (percentage of variegated plants in F1, as detailed earlier) of the chloroplasts "biennis white" and "blandina white" according to Schötz (26) (*SI Appendix, SI Text*). Both crossing series included the same 25 WT chloroplasts, 14 of which had fully sequenced genomes and were employed for correlation mapping (*SI Appendix*, Table S7 and as detailed later). The original data are provided in the study of Schötz (26) and summarized by Cleland (ref. 22, p. 180) and in *SI Appendix*, Table S13. Based on the two transmission frequencies, the WT plastomes were clustered by using the k-means algorithm with Euclidean distance as distance dimension. The optimal number of centers was calculated with the pamk function of the fpc package, as implemented in R v.3.2.1 (67). Strikingly, essentially the same three classes (strong, intermediate, and weak) were obtained that had been previously determined by Schötz (20, 22) (*SI Appendix, SI Text* and Fig. S16).

For the variants, we used the transmission frequencies from I-chi and IV-delta crosses obtained in this work (Fig. 2 and *SI Appendix, SI Text* and Table S10). As the data-driven determination of the optimal number of clusters (k = 2, as detailed earlier) does not reflect the biological situation, upon repeated k-means runs, we chose the number of centers with the best trade-off between lowest swapping rate of the samples between the clusters and the biological interpretability. This approach resulted in four classes (*SI Appendix, SI Text* and Fig. S16).

Correlation Mapping. For correlation mapping in WTs, 14 completely sequenced plastomes (GenBank accession nos. EU262890.2, EU262891.2, KT881170.1, KT881171.1, KT881172.1, KT881176.1, KU521375.1, KX687910.1, KX687913.1, KX687914.1, KX687915.1, KX687916.1, KX687917.1, and KX687918.1) with known inheritance strength (20, 22, 26) (*SI Appendix*, Table S7) were employed. The eight chloroplast genomes assigned to accession numbers starting with KU or KX were newly determined in the course of this work. Mapping of genetic determinants in the green variants was done in 18 fully sequenced mutagenized plastomes (V1a, V1b, V1c, V2a, V2b, V2g, V3a, V3b, V3d, V3e, V3f, V3g, V3h, V4b, V4c, V7a, and VC1) as well as their WT reference (I-johSt; GenBank accession no. AJ271079.4).

In both sequence sets, divergence at a given alignment window was correlated to the experimentally determined inheritance strengths of a chloroplast genome. For the WTs, inheritance strength was measured by using the paternal transmission frequencies (i.e., percentage of variegated plants in the F1) of the chloroplasts biennis white or blandina white according to Schötz (26) (*SI Appendix, SI Text*) or k-means classes combining the two datasets by clustering (*SI Appendix, SI Text* and Table S13 and as described earlier). For the variants, we used the transmission frequencies from the I-chi and IV-delta crosses determined in this work, as well as the k-means classes that were obtained from them (Fig. 2, *SI Appendix, SI Text* and Table S10, and as described earlier).

For correlation of these transmission frequencies to loci on the chloroplast genome, the redundant inverted repeat A (IR$_A$) was removed from all sequences. Then, plastomes were aligned with ClustalW (68) and the alignments were curated manually (*SI Appendix*, Dataset S2). Subsequently, by using a script in R v3.2.1 (67) (*SI Appendix*, Dataset S3), nucleotide changes (SNPs, insertions, and deletions) relative to a chosen reference sequence plastome [I-hookdV (KT881170.1) for WT set and I-johSt (AJ271079.4) for variant set; *SI Appendix, SI Text*] were counted window-wise by two approaches: (i) segmenting the reference sequence in overlapping windows by using a sliding-window approach with a window size of 1 kb and a step size of 10 bp, yielding a matrix of 13,912 × 13 (WT set) and 13,668 × 18 (variants), respectively; or (ii) defining regions of interest with correspondingly chosen window sizes. Then, Pearson's and Spearman's correlation coefficients were calculated between (i) the total count of nucleotide changes for every plastome in the aligned sequence window compared with the reference (i.e., total sequence divergence) and (ii) the determined inheritance strength of the plastomes (*SI Appendix*, Fig. S17 and Dataset S1). For the sliding-window approach, P values were adjusted for multiple testing by using Benjamini–Hochberg correction. To reduce the number of P value adjustments, adjacent alignment windows with identical count vectors were collapsed into one. To annotate the correlation mapping script output file, gene annotation of the consensus sequence (*SI Appendix*, Dataset S2) was converted into bed format (*SI Appendix*, Dataset S3) and combined with the correlation bins by using intersectBed and groupBy of the bedtools package (69). For visualization (Figs. 1A and 3A and *SI Appendix*, Figs. S1 and S10), correlation coefficients obtained for every alignment window were plotted as a function of the alignment position. Correlation values greater than the P value threshold (>0.05) are grayed out. Linear chloroplast genome maps were derived from the annotation of the consensus of both sequence sets (*SI Appendix*, Dataset S2) and drawn by OrganellarGenomeDRAW v1.2 (70) in a linear mode by using a user-defined configuration XML file. Alignments of selected plastome regions were visualized in Geneious v10.2.3 (71) and subsequently, as the output of OrganellarGenomeDRAW, edited in CorelDraw X8 (Corel).

ACCase Activity Assay. ACCase activity was measured in isolated chloroplast suspensions (72, 73) diluted to 400 μg chlorophyll per milliliter (*SI Appendix, Supplementary Materials and Methods*). To validate equilibration to chlorophyll, protein concentration using a Bradford assay (Quick Start Bradford 1× Dye Reagent; Bio-Rad; with BSA solutions of known concentrations as standards) and chloroplast counts per milliliter of suspension were determined for the same samples. For chloroplast counting, the suspension was further diluted 1:10, with 15 μL subsequently loaded on a Cellometer Disposable Cell Counting Chamber (Electron Microscopy Sciences) and analyzed under a Zeiss Axioskop 2 microscope (Zeiss). For each sample, six "B squares" were counted, and chloroplast concentration was calculated as chloroplasts per milliliter = 10 × average count per B square/4 × 10^{-6}. All three equilibration methods gave comparable results.

ACCase activity was measured as the acetyl-CoA–dependent fixation of H^{14}CO$_3^-$ into acid-stable products. For each plant line (I-johSt, V1c, V3e, V2a, V2g, V3d, V3c, VC1, V3g, and IV-atroSt), three independent chloroplast isolations (i.e., three biological replicates) were analyzed in triplicate, including individual negative controls (minus acetyl-CoA) for each measurement. A total of 10 μL of chloroplast suspensions were incubated with 40 μL of reagent solution, with a final concentration of 100 mM Tricine KOH, pH 8.2, 100 mM potassium chloride, 2 mM magnesium chloride, 1 mM ATP, 0.1 mM Triton X-100, 10 mM sodium bicarbonate, 0.5 mM acetyl-CoA, and 40 mM radioactively labeled sodium bicarbonate (NaH^{14}CO$_3$, ca. 4,000 dpm/nmol; Amersham) at room temperature for 20 min. For the negative control, acetyl-CoA in the reaction mixture was replaced by water. Reactions were stopped by adding 50 μL 2 M hydrochloric acid. The sample was transferred to a scintillation vial, and acid labile radioactivity (i.e., remaining H^{14}CO$_3^-$) was evaporated by heating for 20 min at 85 °C. After addition of 3 mL scintillation mixture (Rotiszint eco plus; Carl Roth), the acid-stable radioactivity from incorporation of H^{14}CO$_3^-$ (^{14}C dpm) was detected by liquid

scintillation counter (LS6500; Beckman Coulter). ACCase activity is represented as the ^{14}C incorporation rate into acid-stable fraction (dpm per minute) calculated by dividing the total fixed radioactivity by 20 min. The rates in three replicated reactions were averaged, and corresponding values from negative control samples were subtracted and normalized by the number of chloroplasts to gain ACCase activity in individual samples. The average rates were calculated for each line. To combine all measurements, relative ACCase activities were calculated for each experiment as relative to the I-johSt line, and significant differences between each line and the WT were identified by using a two-tailed paired t test, followed by P value adjustment by using the Benjamini–Hochberg procedure.

Predictability of Inheritance Strength Based on Lipid-Level Data as Explanatory Variables. Lipidomics data from *Oenothera* seedlings of the strain johansen Standard, harboring chloroplast genomes with different assertiveness rates (*SI Appendix, Supplementary Materials and Methods*), were analyzed jointly to test for predictability of inheritance strength based on lipid levels. For this, 33 probes representing 16 genotypes whose chloroplast genomes ranged from inheritance strength class 1 to 5 (*SI Appendix, SI Text*) were measured in five replicates in three independent experimental series (*SI Appendix, SI Text* and Table S3). In this dataset, a total of 184 different lipids/molecules could be annotated (*SI Appendix*, Dataset S4 and as described earlier). To normalize across experiments, the data from each series were log-transformed and median-centered based on genotypes with inheritance strengths of 1, i.e., for every lipid/molecule, its median level across all "inheritance strengths = 1 genotypes" was determined and subtracted from all genotypes tested in the respective experimental series. Inheritance strength 1 was then selected to serve as a common reference across all three experimental series. Subsequently, the three experimental series were combined into a single set. Only those lipids/molecules for which level data were available across all three datasets were considered further, leaving 102 lipids/molecules for analysis (*SI Appendix*, Dataset S4)

LASSO regression model. Inheritance strength was predicted based on the median-centered lipid-level data by using LASSO, a regularized linear regression approach (74), as implemented in the "glmnet" R software package (R v3.2.1) (67). glmnet was invoked with parameter α set to 1 to perform LASSO regression (*SI Appendix*, Dataset S4). The penalty parameter λ was determined from the built-in cross-validation applied to training set data (i.e., all but two randomly selected genotypes) and set to the 1-SE estimate deviation from the optimal (minimal error) value and assuming Gaussian response type. All other parameters were taken as their default values.

Predictive lipids. As a regularized regression method, LASSO aims to use few predictor variables, which allows better identification of truly predictive lipids. Summarized from all 100 cross-validation runs performed, lipids/molecules were ranked by their mean linear model coefficients assigned to them in the LASSO regression, with their absolute value indicating influence strength and their sign indicating positive or negative correlation of their abundance to inheritance strength.

Test for enrichment of predictive lipids/molecules in lipid classes. Across all 100 cross-validation runs, the importance of each of the 102 molecules was assessed based on their average absolute weight factor (avgW) by which they entered the 100 LASSO models. Molecules with avgW of greater than 1 SD obtained across all 102 molecules were considered important. Then, all lipids/molecules were assigned to their respective class (MGDG, DGDG, SQDG, PG, PC, PI, PE, FA, PE, TAG, CoQ, chlorophyll, and pheophytin), and every class was tested for enrichment in the lipid/molecule set considered to be important. This was done by employing a Fisher's exact test, yielding P values and odds ratios. The P values express enrichment, and the odds ratio express the relative enrichment or depletion of a particular class among the set of important lipids.

1. Birky CW, Jr (2001) The inheritance of genes in mitochondria and chloroplasts: Laws, mechanisms, and models. *Annu Rev Genet* 35:125–148.
2. Greiner S, Sobanski J, Bock R (2015) Why are most organelle genomes transmitted maternally? *BioEssays* 37:80–94.
3. Hu Y, Zhang Q, Rao G, Sodmergen (2008) Occurrence of plastids in the sperm cells of *Caprifoliaceae*: Biparental plastid inheritance in angiosperms is unilaterally derived from maternal inheritance. *Plant Cell Physiol* 49:958–968.
4. Birky CW, Jr (1995) Uniparental inheritance of mitochondrial and chloroplast genes: Mechanisms and evolution. *Proc Natl Acad Sci USA* 92:11331–11338.
5. Zhang Q, Sodmergen (2010) Why does biparental plastid inheritance revive in angiosperms? *J Plant Res* 123:201–206.
6. Bendich AJ (2013) DNA abandonment and the mechanisms of uniparental inheritance of mitochondria and chloroplasts. *Chromosome Res* 21:287–296.
7. Reboud X, Zeyl C (1994) Organelle inheritance in plants. *Heredity* 72:132–140.
8. Jansen RK, Ruhlman TA (2012) Plastid genomes of seed plants. *Genomics of Chloroplasts and Mitochondria*, Advances in Photosynthesis and Respiration, eds Bock R, Knoop V (Springer, Dordrecht, The Netherlands), Vol 35, pp 103–126.
9. Barnard-Kubow KB, McCoy MA, Galloway LF (2017) Biparental chloroplast inheritance leads to rescue from cytonuclear incompatibility. *New Phytol* 213:1466–1476.
10. Grun P (1976) *Cytoplasmic Genetics and Evolution* (Columbia Univ Press, New York), 1st Ed, p 446.
11. Hoekstra RF (1990) Evolution of uniparental inheritance of cytoplasmic DNA. *Organizational Constrains of the Dynamics of Evolution*, eds Smith MJ, Vida J (Manchester Univ Press, Manchester, UK), pp 269–278.
12. Cosmides LM, Tooby J (1981) Cytoplasmic inheritance and intragenomic conflict. *J Theor Biol* 89:83–129.
13. Eberhard WG (1980) Evolutionary consequences of intracellular organelle competition. *Q Rev Biol* 55:231–249.
14. Hoekstra RF (2011) Nucleo-cytoplasmic conflict and the evolution of gamete dimorphism. *The Evolution of Anisogamy*, eds Togashi T, Cox PA (Cambridge Univ Press, Cambridge, UK), pp 111–130.
15. Rand DM, Haney RA, Fry AJ (2004) Cytonuclear coevolution: The genomics of cooperation. *Trends Ecol Evol* 19:645–653.
16. Barr CM, Neiman M, Taylor DR (2005) Inheritance and recombination of mitochondrial genomes in plants, fungi and animals. *New Phytol* 168:39–50.
17. Greiner S (2012) Plastome mutants of higher plants. *Genomics of Chloroplasts and Mitochondria*, Advances in Photosynthesis and Respiration, eds Bock R, Knoop V (Springer, Dordrecht, The Netherlands), Vol 35, pp 237–266.
18. De Stordeur E (1997) Nonrandom partition of mitochondria in heteroplasmic *Drosophila*. *Heredity (Edinb)* 79:615–623.
19. Ma H, O'Farrell PH (2016) Selfish drive can trump function when animal mitochondrial genomes compete. *Nat Genet* 48:798–802.
20. Kirk JTO, Tilney-Bassett RAE (1978) *The plastids. Their Chemistry, Structure, Growth and Inheritance* (Elsevier, Amsterdam), 2nd Ed.
21. Schötz F (1954) Über Plastidenkonkurrenz bei *Oenothera*. *Planta* 43:182–240.
22. Cleland RE (1972) *Oenothera–Cytogenetics and Evolution* (Academic, London), 1st Ed, p 370.
23. Gillham NW (1978) *Organelle Heredity* (Raven, New York), 1st Ed, p 602.
24. Stubbe W (1964) The role of the plastome in evolution of the genus *Oenothera*. *Genetica* 35:28–33.
25. Greiner S, Rauwolf U, Meurer J, Herrmann RG (2011) The role of plastids in plant speciation. *Mol Ecol* 20:671–691.
26. Schötz F (1968) Über die Plastidenkonkurrenz bei *Oenothera* II. *Biol Zentralbl* 87:33–61.
27. Kikuchi S, et al. (2013) Uncovering the protein translocon at the chloroplast inner envelope membrane. *Science* 339:571–574.
28. Bölter B, Soll J (2017) Ycf1/Tic214 is not essential for the accumulation of plastid proteins. *Mol Plant* 10:219–221.
29. Salie MJ, Thelen JJ (2016) Regulation and structure of the heteromeric acetyl-CoA carboxylase. *Biochim Biophys Acta* 1861:1207–1213.
30. Chiu W-L, Stubbe W, Sears BB (1988) Plastid inheritance in *Oenothera*: Organelle genome modifies the extent of biparental plastid transmission. *Curr Genet* 13:181–189.
31. Massouh A, et al. (2016) Spontaneous chloroplast mutants mostly occur by replication slippage and show a biased pattern in the plastome of *Oenothera*. *Plant Cell* 28:911–929.
32. Stoike LL, Sears BB (1998) *Plastome mutator*-induced alterations arise in *Oenothera* chloroplast DNA through template slippage. *Genetics* 149:347–353.
33. Sears BB, Stoike LL, Chiu WL (1996) Proliferation of direct repeats near the *Oenothera* chloroplast DNA origin of replication. *Mol Biol Evol* 13:850–863.
34. Chiu W-L, Sears BB (1992) Electron microscopic localization of replication origins in *Oenothera* chloroplast DNA. *Mol Gen Genet* 232:33–39.
35. Wolfe KH (1994) Similarity between putative ATP-binding sites in land plant plastid ORF2280 proteins and the FtsH/CDC48 family of ATPases. *Curr Genet* 25:379–383.
36. De Las Rivas J, Lozano JJ, Ortiz AR (2002) Comparative analysis of chloroplast genomes: Functional annotation, genome-based phylogeny, and deduced evolutionary patterns. *Genome Res* 12:567–583.
37. Langklotz S, Baumann U, Narberhaus F (2012) Structure and function of the bacterial AAA protease FtsH. *Biochim Biophys Acta* 1823:40–48.
38. Kobayashi K, Wada H (2016) Role of lipids in chloroplast biogenesis. *Lipids in Plant and Algae Development*, eds Nakamura Y, Li-Beisson Y (Springer, Cham, Switzerland), pp 103–125.

GENETICS

39. Block MA, Dorne AJ, Joyard J, Douce R (1983) Preparation and characterization of membrane fractions enriched in outer and inner envelope membranes from spinach chloroplasts. II. Biochemical characterization. *J Biol Chem* 258:13281–13286.

40. Botella C, Jouhet J, Block MA (2017) Importance of phosphatidylcholine on the chloroplast surface. *Prog Lipid Res* 65:12–23.

41. Osteryoung KW, Pyke KA (2014) Division and dynamic morphology of plastids. *Annu Rev Plant Biol* 65:443–472.

42. Corriveau JL, Coleman AW (1988) Rapid screening method to detect potential bi-parental inheritacne of plastid DNA and results for over 200 angiosperm species. *Am J Bot* 75:1443–1458.

43. Nishimura Y, Stern DB (2010) Differential replication of two chloroplast genome forms in heteroplasmic *Chlamydomonas reinhardtii* gametes contributes to alternative inheritance patterns. *Genetics* 185:1167–1181.

44. Greiner S, et al. (2008) The complete nucleotide sequences of the five genetically distinct plastid genomes of *Oenothera*, subsection *Oenothera*: I. Sequence evaluation and plastome evolution. *Nucleic Acids Res* 36:2366–2378.

45. Wicke S, Schneeweiss GM, dePamphilis CW, Müller KF, Quandt D (2011) The evolution of the plastid chromosome in land plants: Gene content, gene order, gene function. *Plant Mol Biol* 76:273–297.

46. de Vries J, Sousa FL, Bölter B, Soll J, Gould SB (2015) YCF1: A green TIC? *Plant Cell* 27:1827–1833.

47. Bölter B, Soll J (2016) Once upon a time–Chloroplast protein import research from infancy to future challenges. *Mol Plant* 9:798–812.

48. Jansen RK, et al. (2007) Analysis of 81 genes from 64 plastid genomes resolves relationships in angiosperms and identifies genome-scale evolutionary patterns. *Proc Natl Acad Sci USA* 104:19369–19374.

49. Wicke S, Naumann J (2018) Molecular evolution of plastid genomes in parasitic flowering plants. *Advances in Botanical Research*, eds Chaw S-M, Jansen RK (Academic, New York), Vol 85, pp 315–347.

50. Newton WCF (1931) Genetical experiments with *Silene otites* and related species. *J Genet* 24:109–120.

51. Rockenbach K, et al. (2016) Positive selection in rapidly evolving plastid-nuclear enzyme complexes. *Genetics* 204:1507–1522.

52. Barnard-Kubow KB, Sloan DB, Galloway LF (2014) Correlation between sequence divergence and polymorphism reveals similar evolutionary mechanisms acting across multiple timescales in a rapidly evolving plastid genome. *BMC Evol Biol* 14:268.

53. Bogdanova VS, Galieva ER, Kosterin OE (2009) Genetic analysis of nuclear-cytoplasmic incompatibility in pea associated with cytoplasm of an accession of wild subspecies *Pisum sativum* subsp. *elatius* (Bieb.) Schmahl. *Theor Appl Genet* 118:801–809.

54. Bogdanova VS, et al. (2015) Nuclear-cytoplasmic conflict in pea (*Pisum sativum* L.) is associated with nuclear and plastidic candidate genes encoding acetyl-CoA carboxylase subunits. *PLoS One* 10:e0119835.

55. Ulbricht-Jones ES (2017) The virescent and narrow leaf phenotype of a plastome-genome-incompatible *Oenothera* hybrid is associated with the plastid gene *accD* and fatty acid synthesis. PhD thesis (Univ Potsdam, Potsdam, Germany).

56. Dietrich W, Wagner WL, Raven PH (1997) *Systematics of Oenothera Section Oenothera Subsection Oenothera (Onagraceae)* (American Society of Plant Taxonomists, Laramie, WY), 1st Ed, p 234.

57. Greiner S, Köhl K (2014) Growing evening primroses (*Oenothera*). *Front Plant Sci* 5:38.

58. Harte C (1994) *Oenothera–Contributions of a Plant to Biology* (Springer, Berlin), 1st Ed.

59. Cleland RE (1935) Cyto-taxonomic studies on certain Oenotheras from California. *Proc Am Philos Soc* 75:339–429.

60. Stubbe W (1989) *Oenothera*–An ideal system for studying the interaction of genome and plastome. *Plant Mol Biol Rep* 7:245–257.

61. Kutzelnigg H, Stubbe W (1974) Investigation on plastome mutants in *Oenothera*: 1. General considerations. *Subcell Biochem* 3:73–89.

62. Stubbe W, Herrmann RG (1982) Selection and maintenance of plastome mutants and interspecific genome/plastome hybrids from Oenothera. *Methods in Chloroplast Molecular Biology*, eds Edelman M, Hallick RB, Chua N-H (Elsevier, Amsterdam), pp 149–165.

63. Epp MD (1973) Nuclear gene-induced plastome mutations in *Oenothera hookeri*: I. Genetic analysis. *Genetics* 75:465–483.

64. Chang T-L, et al. (1996) Characterization of primary lesions caused by the plastome mutator of *Oenothera*. *Curr Genet* 30:522–530.

65. Chiu W-L, et al. (1990) *Oenothera* chloroplast DNA polymorphisms associated with plastome mutator activity. *Mol Gen Genet* 221:59–64.

66. Sears BB, Sokalski MB (1991) The *Oenothera* plastome mutator: Effect of UV irradiation and nitroso-methyl urea on mutation frequencies. *Mol Gen Genet* 229:245–252.

67. R Core Team (2015) R: A Language and Environment for Statistical Computing. Version 3.2.1 (R Foundation for Statistical Computing, Vienna).

68. Thompson JD, Higgins DG, Gibson TJ (1994) CLUSTAL W: Improving the sensitivity of progressive multiple sequence alignment through sequence weighting, position-specific gap penalties and weight matrix choice. *Nucleic Acids Res* 22:4673–4680.

69. Quinlan AR, Hall IM (2010) BEDTools: A flexible suite of utilities for comparing genomic features. *Bioinformatics* 26:841–842.

70. Lohse M, Drechsel O, Kahlau S, Bock R (2013) OrganellarGenomeDRAW–A suite of tools for generating physical maps of plastid and mitochondrial genomes and visualizing expression data sets. *Nucleic Acids Res* 41:W575–W581.

71. Kearse M, et al. (2012) Geneious Basic: An integrated and extendable desktop software platform for the organization and analysis of sequence data. *Bioinformatics* 28:1647–1649.

72. Hunter SC, Ohlrogge JB (1998) Regulation of spinach chloroplast acetyl-CoA carboxylase. *Arch Biochem Biophys* 359:170–178.

73. Thelen JJ, Ohlrogge JB (2002) The multisubunit acetyl-CoA carboxylase is strongly associated with the chloroplast envelope through non-ionic interactions to the carboxyltransferase subunits. *Arch Biochem Biophys* 400:245–257.

74. Tibshirani R (1996) Regression shrinkage and selection via the Lasso. *J R Stat Soc B* 58:267–288.

75. Hirata N, Yonekura D, Yanagisawa S, Iba K (2004) Possible involvement of the 5′-flanking region and the 5′UTR of plastid accD gene in NEP-dependent transcription. *Plant Cell Physiol* 45:176–186.

76. Hajdukiewicz PT, Allison LA, Maliga P (1997) The two RNA polymerases encoded by the nuclear and the plastid compartments transcribe distinct groups of genes in tobacco plastids. *EMBO J* 16:4041–4048.

77. Swiatecka-Hagenbruch M, Liere K, Börner T (2007) High diversity of plastidial promoters in *Arabidopsis thaliana*. *Mol Genet Genomics* 277:725–734.

78. Kozaki A, Mayumi K, Sasaki Y (2001) Thiol-disulfide exchange between nuclear-encoded and chloroplast-encoded subunits of pea acetyl-CoA carboxylase. *J Biol Chem* 276:39919–39925.